JOURNAL OF MATERIALS SCIENCE 11 (1976) 2247–2257

Behaviour of non-coaxial dislocation loops in ordered alloys

K. SADANANDA
Engineering Materials Group, and Department of Mechanical Engineering, University of Maryland, College Park, Maryland, USA

A detailed numerical analysis of the behaviour of non-coaxial superlattice dislocation loops lying on parallel slip planes has been made by approximating the loops in terms of piecewise segments. There are several competitive processes that could occur between the loops. These include, complete passing of the loops over one another, partial passing of the loops that leads to uncoupling of the loops and thus to disorder in the crystal, elongation of the loops that leads to the formation of long screw dipoles, and finally cross-slip of the loops that leads to mutual annihilation of unlike screw segments by any of four alternate modes of cross-slip involving one or both dislocation loops. Among these several paths, the one that has the lowest energy is determined for various loop sizes and their spacings. The results show that, depending upon the interplanar separation, Z, the loops either pass one another, or else elongate preferentially along their screw orientation until sufficient internal stresses are developed to cause them to cross-slip. However, no uncoupling of the dislocation loops is observed.

1. Introduction

One of the significant effects of atomic ordering in alloys is the change in their dislocation morphology. Hitherto perfect dislocations in disordered alloys become imperfect upon ordering and become attached to a plane of antiphase boundary (APB). The existence of superlattice dislocation, which is simply a pair of these imperfect dislocations coupled by a finite width of APB, therefore becomes a necessity in ordered alloys in order to minimize this APB energy. Because of these changes in the dislocation morphology, atomic ordering has a profound effect on the mechanical properties of alloys (see [1] for a review). In particular, even the single crystalline ordered alloys [2–5] that are oriented for single slip show significant work-hardening with the work-hardening rates approaching nearly one tenth of the shear modulus. Associated with these high work-hardening rates is the generation of slip-induced disorder which occurs to the extent that at large strains corresponding to stage III deformation the stress–strain curves of these ordered alloys become similar to those of their corresponding disordered alloys. This essentially implies that superlattice dislocations at these large strains become uncoupled and hence behave similar to dislocations in disordered alloys. It is therefore imperative to incorporate a mechanism for the generation of disorder in any work-hardening model for ordered alloys.

Various dislocation models have been proposed to account for this slip-induced disorder which include the APB tube model [5–8] as well as the dipole model [9] involving the elastic interaction of passing superlattice dislocations on parallel slip planes, that is the Taylor model [10]. APB tube generation requires intersecting slip systems [5] and, therefore, does not account for the high work-hardening rates observed in single crystalline ordered alloys oriented for single slip. The dipole model, on the other hand, is most likely to be applicable for single slip orientations and is based on many experimental observations which show the presence of abundant numbers of dislocation dipoles [2–4]. The uncoupling of superlattice dislocations by this model, however, does not occur until the separation between the passing dislocations is below some critical value [9]. But recent calculations [11] indicate that such small separations between the passing dislocations may not be reached, especially if the dislocations are of pure screw type, since these dislocations could easily cross-slip under their own internal stresses and mutually annihilate one another. The above mentioned calculations, however, have been based on the infinite dislocation line approximation, whereas the dislocations in real crystal generally consist of irregularly shaped loops of finite dimensions. In order to understand the behaviour of these loops, a detailed analysis of the cross-slip behaviour of non-coaxial dislocation loops on parallel slip planes facing their screw segments has been made recently [12]. An understanding of the behaviour of these non-coaxial dislocation loops is important since they approximate the situation wherein the dislocation loops are nucleated at various points inside the crystal and expand until they meet one another. Among other things, the above analysis showed that it is possible to obtain much smaller separation between passing dislocation loops without them undergoing cross-slip and mutual annihilation since cross-slip of these dislocation loops is considerably more difficult because of their line tension. This difficulty is even more pronounced when the loop size is small.

In the above calculations [12], it was not possible to determine whether or not such small separations between the dislocation loops are sufficient to uncouple the loops during their passing. This is because the above analysis considered only one or two dislocation loops which do not pass one another in an otherwise perfect crystal. The result was that the segments of the loops that face each other form dipoles while the remainder of the segments expand into the crystal. In order to force the dislocation loops to pass one another, it is necessary, then, to consider the presence of other dislocation loops in the neighbourhood which restrict the unlimited free expansion of the dislocation loops under consideration. The presence of these neighbouring loops can be taken into consideration by viewing them as forming an infinite array of non-coaxial dislocations loops, all lying on parallel slip planes. Among the various possible arrays, we shall consider, for simplicity, a two-dimensional array wherein the axis of the loops lie on the same plane. This array is similar to that considered earlier [13], where it was shown that the most important effect of the presence of the other loops in the neighbourhood is to constrain each loop to be symmetric, i.e. the opposite segments of each loop are separated symmetrically from the centre of the loop. In addition to passing, the specific choice of the constraints also allows the loops to expand preferentially along screw orientations, thereby generating elongated loops in agreement with many experimental observations [2–4]. In the following sections, we shall examine the passing as well as the cross-slip behaviour of these constrained dislocation loops and determine the conditions under which the loops could be uncoupled to generate disorder in the crystal.

2. Constrained dislocation loops

Fig. 1a shows the piecewise approximation of two non-coaxial dislocation loops on parallel slip planes which expand towards one another along their screw segments. The two loops considered are assumed to be part of an infinite array of such loops discussed above. While considering only two loops of the array, it is assumed again that the remainder of the loops have no significant effect on the equilibrium shapes of the two loops, other than imposing the specific constraints discussed above. That the above assumption is justified has already been shown earlier [13].

The equilibrium configuration of the two loops in Fig. 1a is given by a complex saddle point type of position on a multi-dimensional energy surface determined by variables R_1, R_2, R_3 and R_4. In addition to these variables, the total energy of the loops also depends on Y, Z and τ, where Y is the separation between the axes of the loops, Z is the vertical separation between the slip planes containing the loops and τ is the applied stress necessary to keep the loops in equilibrium. In order to facilitate easy comparison of the equilibrium configuration of the loops with those of infinite dislocations, the projection of the opposite screw segments that form dipoles is also shown on the right-hand side of Fig. 1a, where X_0 and X_1 define the relative positions of these segments and are given by

$$X_0 = \frac{R_4 - Y}{2} \tag{1}$$

$$X_1 = \frac{R_2 - R_4}{2}, \tag{2}$$

where X_0 is defined as positive when segment 12 is to the left of segment 6 (Fig. 1a) and as negative otherwise. The total energy of the two loops is given by

$$E_{\mathrm{T}} = E_{\mathrm{S}}^{\mathrm{I}} + E_{\mathrm{S}}^{\mathrm{II}} + E_{\mathrm{S}}^{\mathrm{III}} + E_{\mathrm{S}}^{\mathrm{IV}} + E_{\mathrm{I}}^{\mathrm{I-II}} + E_{\mathrm{I}}^{\mathrm{I-III}} + E_{\mathrm{I}}^{\mathrm{I-IV}} + E_{\mathrm{I}}^{\mathrm{II-III}} + E_{\mathrm{I}}^{\mathrm{II-IV}} + E_{\mathrm{I}}^{\mathrm{III-IV}} + E_{\tau} + E_{\gamma} \quad (3)$$

where superscripts I, II etc. refer to dislocation loops I, II, etc. and subscripts S and I refer to self energy of a loop and interaction energy between two loops, respectively. The individual energy terms on the right-hand side of Equation 3 can be expanded in terms of the piecewise segments in Fig. 1a. Since these expressions are somewhat lengthy, such an expansion is given below for the simple configuration of Fig. 1a. Based on these, one can easily deduce the expressions for other loop configurations that are discussed in this paper. The above energy terms are given by

$$E_{\mathrm{S}}^{\mathrm{I}} = E_{\mathrm{S}}^{\mathrm{III}} = 2E_{\mathrm{S}}^{1} + 2E_{\mathrm{S}}^{2} + E_{\mathrm{I}}^{1-3} + E_{\mathrm{I}}^{2-4} \quad (4)$$

$$E_{\mathrm{S}}^{\mathrm{II}} = E_{\mathrm{S}}^{\mathrm{IV}} = 2E_{\mathrm{S}}^{5} + 2E_{\mathrm{S}}^{6} + E_{\mathrm{I}}^{5-7} + E_{\mathrm{I}}^{6-8} \quad (5)$$

$$E_{\mathrm{I}}^{\mathrm{I-II}} = E_{\mathrm{I}}^{\mathrm{III-IV}} = 2(E_{\mathrm{I}}^{1-5} + E_{\mathrm{I}}^{1-7} + E_{\mathrm{I}}^{2-6} + E_{\mathrm{I}}^{2-8}) \quad (6)$$

$$E_{\mathrm{I}}^{\mathrm{I-III}} = 2(E_{\mathrm{I}}^{1-9} + E_{\mathrm{I}}^{1-11} + E_{\mathrm{I}}^{2-10}) + E_{\mathrm{I}}^{2-12} + E_{\mathrm{I}}^{4-10} \quad (7)$$

$$E_{\mathrm{I}}^{\mathrm{I-IV}} = E_{\mathrm{I}}^{\mathrm{II-III}} = 2(E_{\mathrm{I}}^{1-13} + E_{\mathrm{I}}^{1-15} + E_{\mathrm{I}}^{2-14}) + E_{\mathrm{I}}^{2-16} \quad (8)$$

$$E_{\mathrm{I}}^{\mathrm{II-IV}} = 2(E_{\mathrm{I}}^{5-13} + E_{\mathrm{I}}^{5-15} + E_{\mathrm{I}}^{6-14}) + E_{\mathrm{I}}^{6-16} + E_{\mathrm{I}}^{8-14} \quad (9)$$

where the self energy of segment i is denoted by E_{S}^{i} while the interaction energy between segments i and j is denoted by E_{I}^{i-j}. These energies are determined using the expressions developed by Jossang and his co-workers [14–16]. The last two terms in Equation 3 are the work done by the applied stress and the work expended in creating γ, the APB energy, respectively and these in turn are given by

$$E_{\tau} = -2\tau b(R_1R_2 + R_3R_4) \quad (10)$$

and

$$E_{\gamma} = 2\gamma(R_1R_2 - R_3R_4). \quad (11)$$

The configuration of the dislocation loops after complete passing is shown in Fig. 1b. Since all of the segments in the piecewise approximation remain the same as in Fig. 1a, the total energy of the loops is the same as that given by Equations 3 to 11. The projection of the screw segments on the right-hand side of Fig. 1b shows that complete passing of the loops is characterized by an increase of X_0 without a corresponding increase in X_1. As will be shown later, when the loops pass one another, the relative contribution from the interaction energy between the two loops to the total energy decreases to the extent that the loops behave as independent of one another, i.e. as single superlattice dislocation loops.

Fig. 1c, on the other hand, shows the configuration of the loops after partial passing of the loops wherein only the outer loops pass one another leaving the inner loops locked as a dipole. The position of the screw segments shown on the right hand side indicates that this configuration corresponds to the uncoupling of the superlattice dislocations discussed earlier [9]. In comparison to complete passing, the uncoupling of the loops is characterized by the simultaneous increase of X_0 and X_1 as shown in Fig. 1c.

There is a third alternate path that the dislocation loops can take and this is shown in Fig. 1d. In this case the applied stress is smaller than that required for passing, but is sufficient to expand the loops at least along one direction. Since the dislocation loops are constrained not to expand along R_2 direction except by way of "passing", they expand only along R_1 direction. Such an expansion gives rise to elongated loops with long screw dipoles, a common feature observed in single crystalline ordered alloys [2–4]. This particular expansion of the loops is characterized by the increase of R_1 and R_3 without a corresponding increase in R_2 and R_4 (Fig. 1a) and furthermore such an expansion has no counterpart in terms of infinite dislocation behaviour.

3. Cross-slip configurations

If the internal stresses due to each loop are of sufficient magnitude the dislocation loops instead could cross-slip towards one another and mutually annihilate their unlike screw segments. Thus cross-slip of the loops provides an alternate path to passing, uncoupling or elongation. There are, however, four alternate modes by which cross-slip of the loops could be accomplished and these are

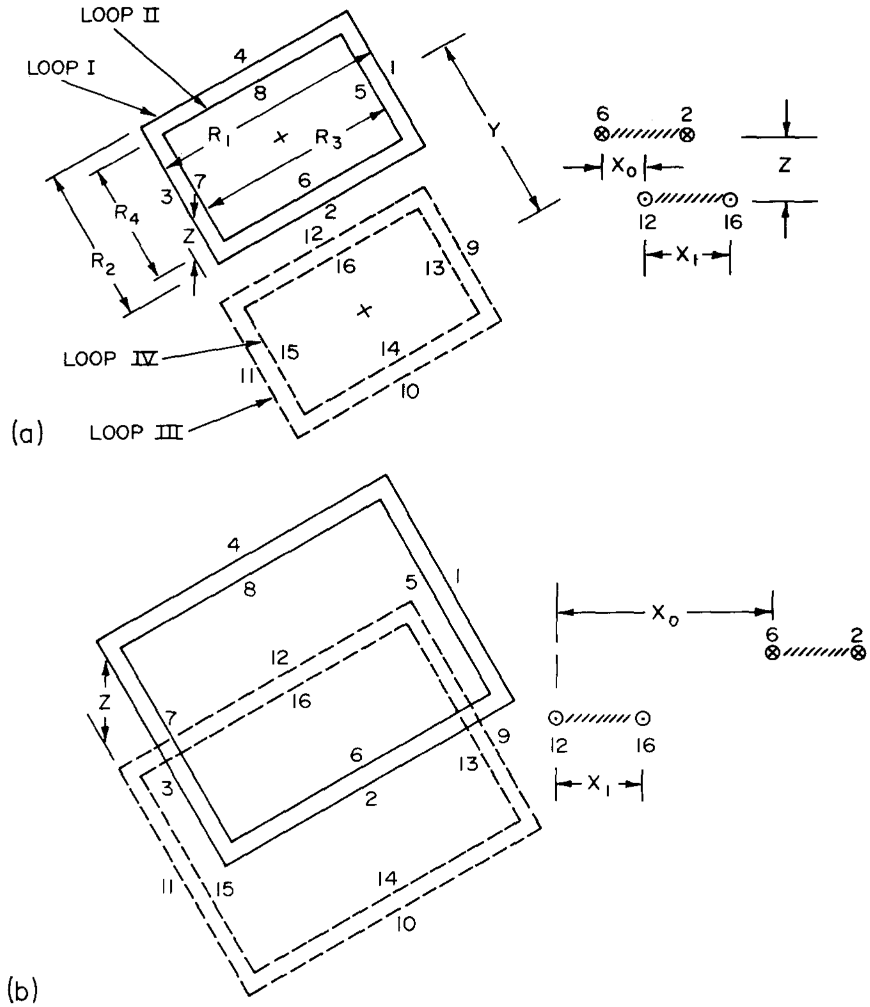

Figure 1 (a) Two constrained non-coaxial passing superlattice dislocation loops on parallel slip planes meeting one another along their screw segments. (b) The loops passing one another. (c) Outer dislocation loops pass one another leaving the inner loops remain locked as a dipole thereby causing partial uncoupling of the superlattice dislocation loops. (d) Elongation of the dislocation loops along screw direction thereby generating long screw dipoles.

shown in Fig. 2. Fig. 2a and b show somewhat symmetric cross-slip wherein both loops simultaneously cross-slip towards one another. In particular, Fig. 2a shows the two outer loops symmetrically cross-slipping on a plane joining them, which makes an angle α with the primary plane. The total energy of the loops is given by Equation 3 wherein the work done by the applied stress and by the APB tension is given by

$$E_\tau = -2\tau b(R_1R_2 + R_3R_4) + 2\tau b \cos\alpha\, R_1 d \quad (12)$$

$$E_\gamma = 2\gamma(R_1R_2 - R_3R_4) + 2\gamma(R_1R_2 - R_3R_4) + 2\gamma R_1 d \quad (13)$$

where it is assumed, for simplicity, that the APB energy, γ, is the same on both the primary and cross-slip planes. Also, in all the figures that follow, the extent of cross-slip of a given loop is denoted by d.

The second mode of symmetric cross-slip is shown in Fig. 2b, wherein the two inner loops cross-slip simultaneously towards one another. The work done by the applied stress and the APB tension, however, are given by

$$E_\tau = -2\tau b(R_1R_2 + R_3R_4) - 2\tau b \cos\alpha\, R_3 d \quad (14)$$

$$E_\gamma = 2\gamma(R_1R_2 - R_3R_4) + 2\gamma R_3 d. \quad (15)$$

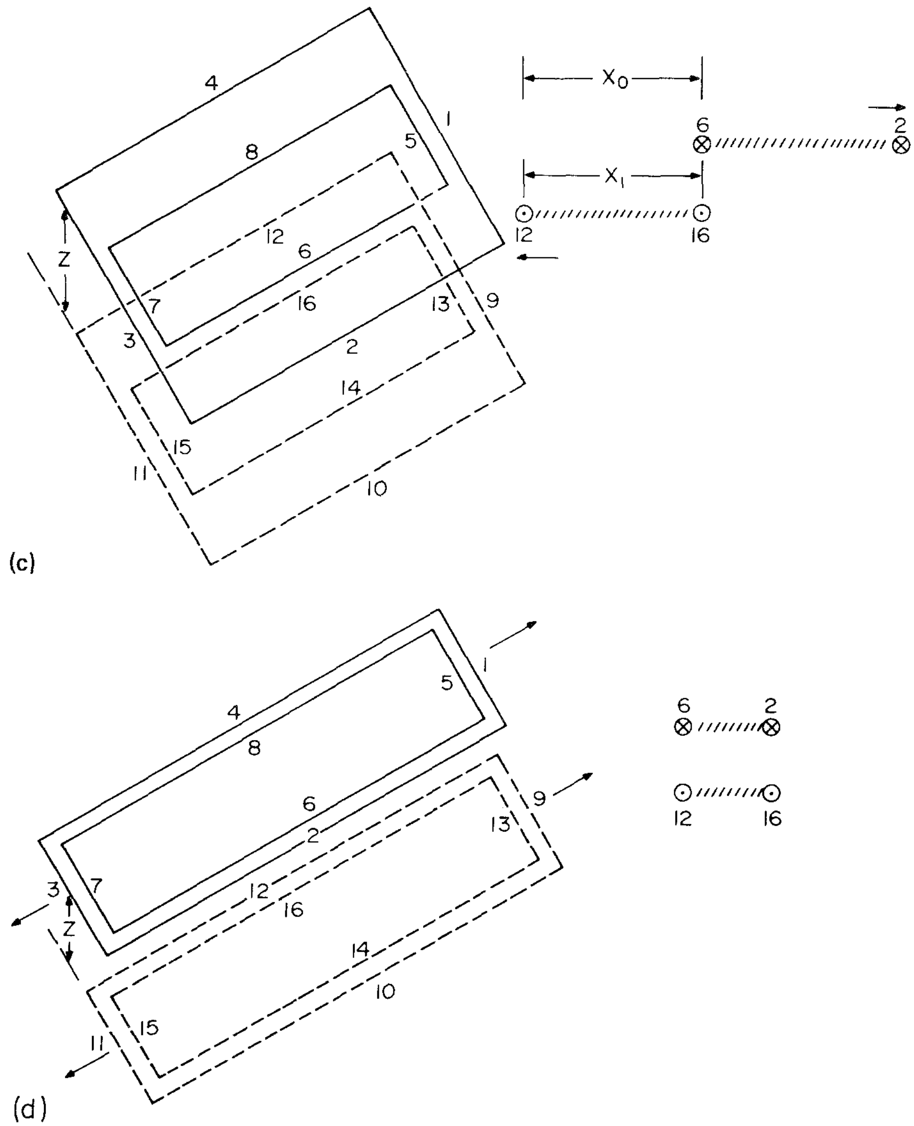

Figure 1 continued.

For infinite dislocations, the configurations in Fig. 2a and b reduce to one since there is no distinction between outer and inner dislocations.

Among asymmetric modes, Fig. 2c shows the cross-slip of only one inner dislocation loop towards the outer loop of the other superlattice dislocation loop. The work done by the applied stress and the APB tension for this case are given by

$$E_\tau = -2\tau \boldsymbol{b}(R_1R_2+R_3R_4)+\tau \boldsymbol{b}\cos\alpha\, R_3 d \tag{16}$$

$$E_\gamma = 2\gamma(R_1R_2-R_3R_4)+\gamma R_3 \boldsymbol{b}. \tag{17}$$

Finally, the second asymmetric cross-slip mode is represented by Fig. 2d wherein only one outer loop cross slips towards the inner loop of other superlattice dislocation loop. The work done by the applied stress and by the APB tension for this case is given by

$$E_\tau = -2\tau \boldsymbol{b}(R_1R_2+R_3R_4)+\tau \boldsymbol{b}\cos\alpha\, R_1 d \tag{18}$$

$$E_\gamma = 2\gamma(R_1R_2-R_3R_4)+\gamma R_1 d. \tag{19}$$

Except for the fact that there are two symmetric cross-slip modes, the configurations in Fig. 2 are

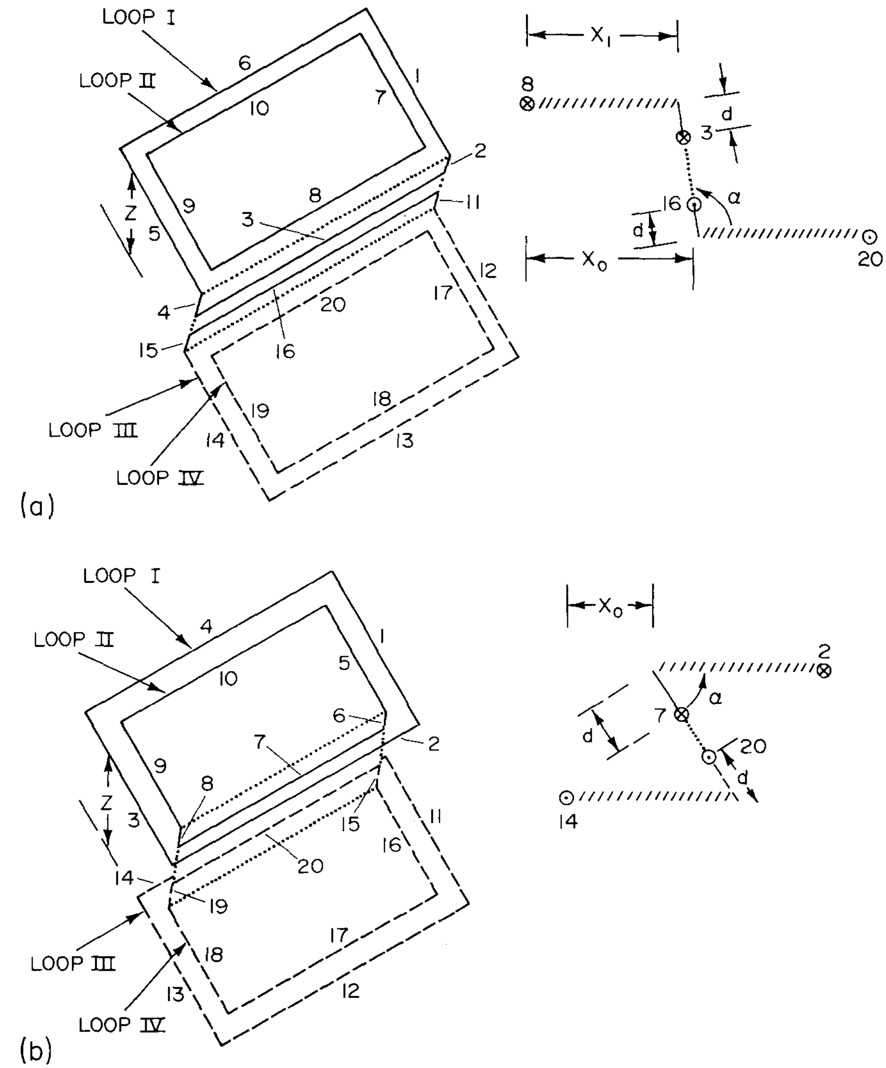

Figure 2 Cross-slip of non-coaxial dislocation loops (a) symmetric cross-slip involving outer dislocation loops, (b) symmetric cross-slip involving inner dislocation loops. (c) Asymmetric cross-slip involving only one inner dislocation loop. (d) Asymmetric cross-slip involving only one outer dislocation loop. Dotted planes represent the cross slip planes.

similar to those considered with reference to infinite superlattice dislocations [11].

For any given cross-slip mode, the total energy of the cross-slipping dislocation loops varies with the cross-slip distance as shown schematically in Fig. 3. In particular, for Z less than Z_3, cross-slip occurs spontaneously and correspondingly the total energy decreases continuously with the distance. However, at slightly larger values of Z, the energy–distance curves show a small minimum before they pass through a maximum. The minimum generally occurs when d is of the order of 1 to 5 Å. At still slightly larger values of Z the energy increases continuously with distance without going through any observable minimum. These energy–distance curves are similar to those determined earlier for unconstrained non-coaxial dislocation loops. In order to check whether the loops of a given configuration cross-slip spontaneously or not, cross-slip energies have to be determined for each one of the four cross-slip modes. To minimize the computational time involved, the following procedure, however, is adopted. Instead of determining the complete energy–distance curves, the cross-slip energies for each mode are determined at three values of d, each of 4 Å separation. Spontaneous cross-slip by the given mode is allowed to occur if cross-

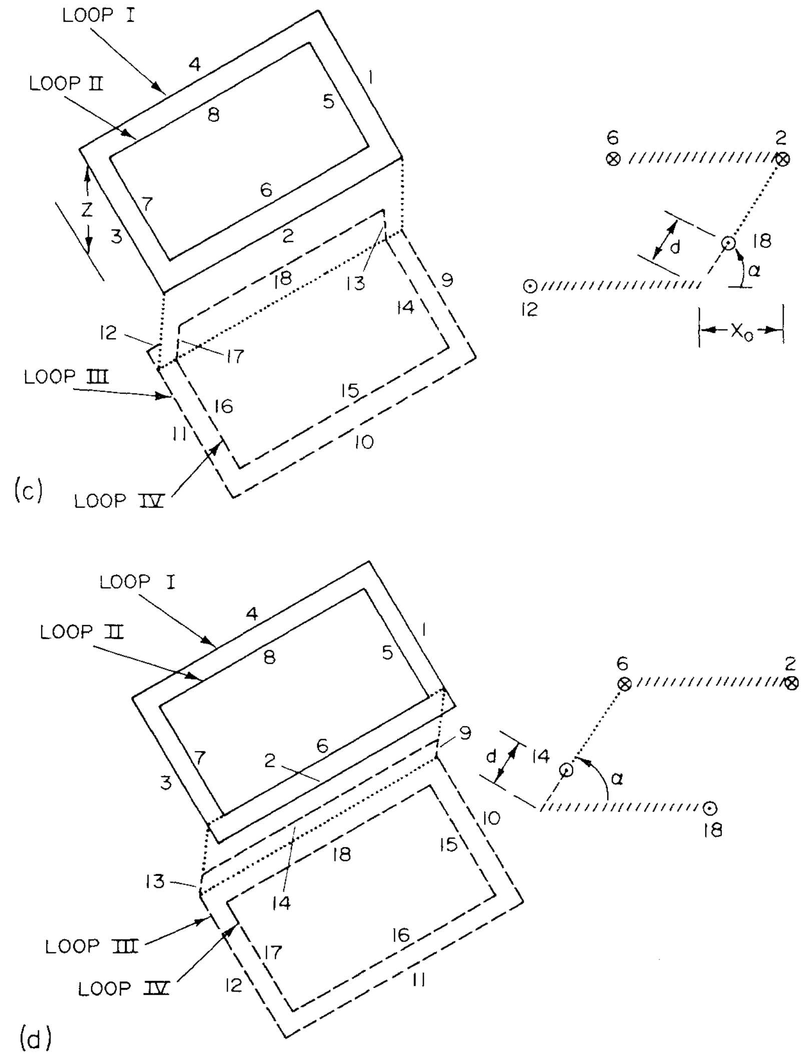

Figure 2 continued.

slip energies for the three successive values of d decrease continuously. It is necessary to select at least three values to make sure that the cross-slip energy decreases continuously rather than shows a minimum. This procedure is somewhat similar to the more simplified procedure adopted for infinite dislocations [11], wherein the above complexities such as a minimum followed by a maximum do not exist.

4. Results

The typical behaviour of non-coaxial dislocation loops is shown in Fig. 4 and it is compared with that of single loops in ordered alloys. The solid curves in this figure represent the equilibrium configurations of single superlattice dislocation loops as well as single outer dislocation loops enclosing APB. For simplicity, the variation of only R_1 with the stress is presented in Fig. 4. Because of computational difficulties in determining the equilibrium configurations of the single superlattice dislocation loops at high stresses, its curves is simply extrapolated to meet the curve of the outer loop and such an extrapolation seems justified on the basis of the previous results obtained on circular dislocation loops [17]. In keeping with previous studies, the present calculations have been performed using the material

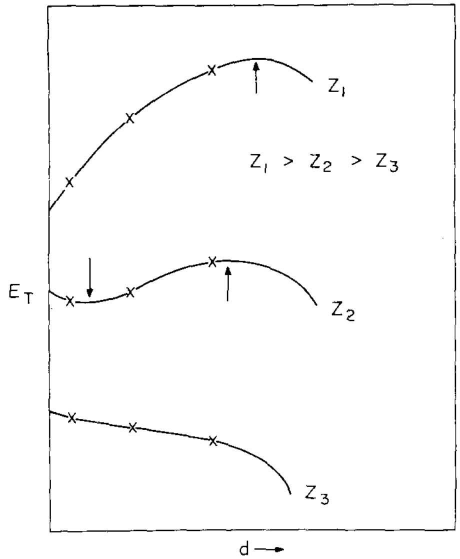

Figure 3 A schematic illustration showing the variation of the energy of cross slipping dislocation loops as a function of the cross-slip distance for any one of the cross-slip modes discussed in Fig. 2.

constants corresponding to a fully ordered FeCo alloy [1]. In particular $\mu = 7 \times 10^{11}\,\text{dyn cm}^{-2}$, $b = 2.47 \times 10^{-8}\,\text{cm}$, $\nu = 1/3$, and $\gamma_{(110)} = 157\,\text{erg cm}^{-2}$ have been used.

The bahaviour of non-coaxial dislocation loops is shown by dash–dot curves in Fig. 4. Since the loop behaviour is most pronounced when the loop size is small, attention is focused on the behaviour of the smallest size superlattice dislocation loops that could be obtained. Fig. 4, in particular, illustrates the behaviour of loops with $y = 300 \times 10^{-8}\,\text{cm}$. The loops essentially behave as single superlattice dislocation loops until they meet one another. The behaviour of the loops after their screw segments meet one another depends on Z. For example, for $Z = 50 \times 10^{-8}\,\text{cm}$; the results show that R_1 increases with a decrease in stress at much faster rate than that of single loops. This implies that the loops are becoming much more elliptical than that of single loops, that is the loops elongate preferentially along their screw orientation and the configuration corresponds to that shown in Fig. 1d. Because of the small value of Z, the applied stress apparently is not high enough for the loops to pass one another breaking their dipole configuration. Also, because of the small value of Z, the total energy per unit length of the dipole is small, and the loops could preferentially elongate along the R_1 direction. Since

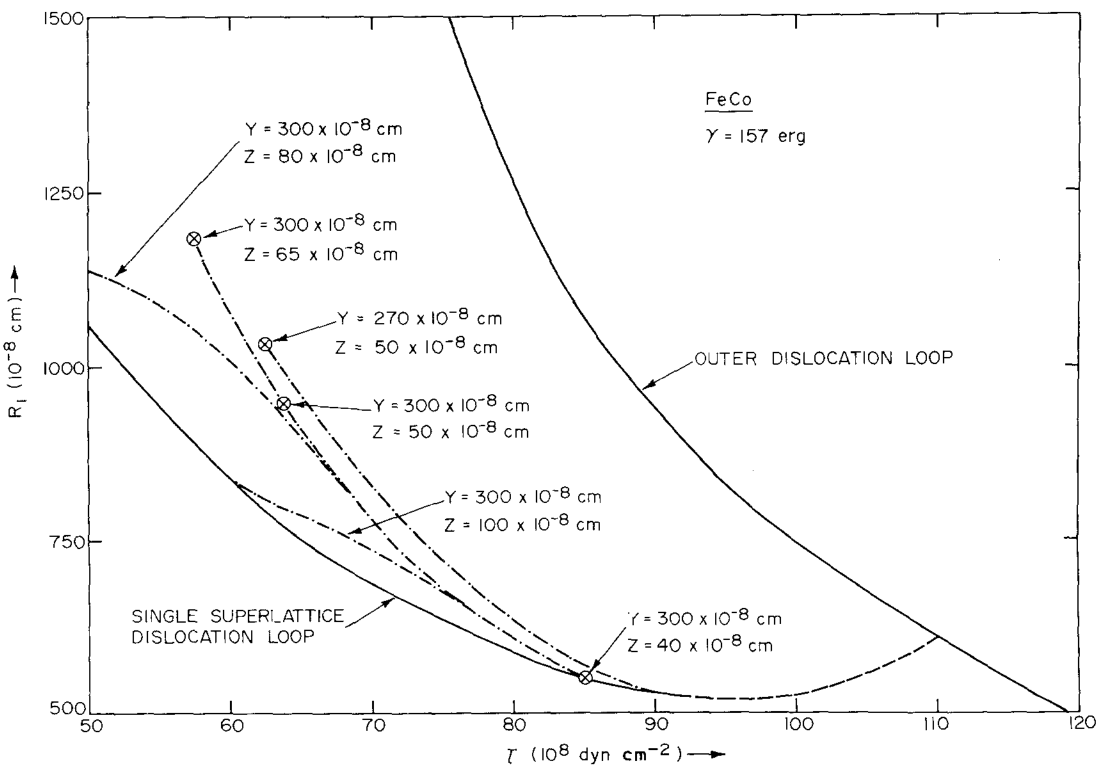

Figure 4 Equilibrium configurations of non-coaxial superlattice dislocation loops.

the dipole is stable, the lowest energy equilibrium during such elongation corresponds to a saddle point on the total energy surface involving the energy minimum in terms of R_2, R_3 and R_4 and maximum in terms of R_1. During passing, however, the dipole configuration becomes unstable and the equilibrium configuration during such passing is found to correspond to a minimum in terms of R_1, R_3 and R_4 and a maximum in terms of R_2. Determination of these complex saddle points, however, involves many steps and they have been illustrated earlier [18] with reference to hexagonal loops. The configurations represented in Fig. 4, correspond to these saddle point configurations determined for each decrease in stress. After determining the equilibrium configuration for a given stress, the configuration is tested for cross-slip by all of the four modes discussed earlier. This test again involves the determination of the changes in the saddle point configurations as the cross-slip distance d is increased from zero as discussed in the previous section.

The results for $Y = 300 \times 10^{-8}$ cm and $Z = 50 \times 10^{-8}$ show that cross-slip of the loops does not occur until R_1 is increased to 950×10^{-8} cm. When Z is increased to 65×10^{-8} cm, the loops follow essentially the same path as before, except that the loops elongate to a larger distance before they cross-slip. Since Z is larger, the cross-slip forces between the loops are reduced and the only way to increase these forces is to generate longer dipoles. The cross-slip in both cases is found to occur by mode b (Fig. 2b).

When Z is further increased to 80×10^{-8} cm, the dipole, however, is no longer stable and passing becomes a competitive process with respect to elongation and to cross-slip. Fig. 4 shows that for this value of Z, the loops start to pass one another after their some initial elongation. This passing is accompanied by the bending of the $R_1 - \tau$ curve towards the single loop curve, and ultimately when the loops pass one another, the two curves converge to one and this aspect can be seen more clearly for $Z = 100 \times 10^{-8}$ cm. That is, the loops behave essentially as independent loops after they pass one another. With an increase of Z to infinity, the equilibrium configurations of the loops should follow the solid curve for all stresses since the loops are independent of each other. On the other hand, when Z is decreased from 50×10^{-8} cm to 40×10^{-8} cm, cross-slip of the loops occurs at a smaller R_1 value and in fact cross-slip occurs immediately after the loops meet one another as shown in Fig. 4. At these smaller values of Z, cross-slip is found to occur by mode a (Fig. 2a) that is for these Z values, cross-slip occurs as soon as the outer loops meet one another.

It is next of importance to consider the effect of Y on the behaviour of the loops. When Y is decreased to 270×10^{-8} cm and with Z remaining the same as 50×10^{-8} cm, the results show that the loops have to elongate to larger value of R_1 before they cross-slip. Since a decreasing Y reduces R_2 and R_4, the loops have to overcome larger line tensions before they can cross-slip. Another effect of the decrease of Y is to shift the $R_1 - \tau$ curve to higher stress. This is again related to the fact that due to the smaller radius, the loops have to expend more energy to elongate along the R_1 direction. Except for the above differences, the results for $Y = 270 \times 10^{-8}$ cm are found to be similar to those for $Y = 300 \times 10^{-8}$ cm.

The present calculations also showed that it is difficult to decrease Y any smaller than $Y = 270 \times 10^{-8}$ cm since for Y less than 270×10^{-8} cm, superlattice dislocation loops become unstable due to the collapse of the inner loops. Hence, for Y less than 270×10^{-8} cm the dislocation loops meet as outer loops as shown in Fig. 5. The behaviour of these loops is similar to that of the unextended dislocation loops determined earlier [19] except that the APB energy in the present case acts somewhat similar to a frictional force. Thus depending on the value of Z, the loops either elongate along the R_1 direction, or cross-slip and annihilate their screw segments, or else pass one another if Z is sufficiently large. When they cross-slip or elongate along the R_1 direction,

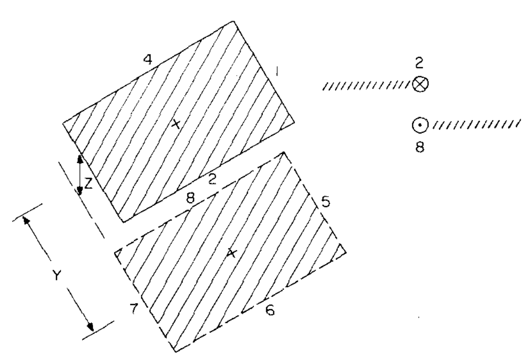

Figure 5 Collapse of the inner dislocation loops occurs when Y is small leaving the outer loops alone thereby generating disorder.

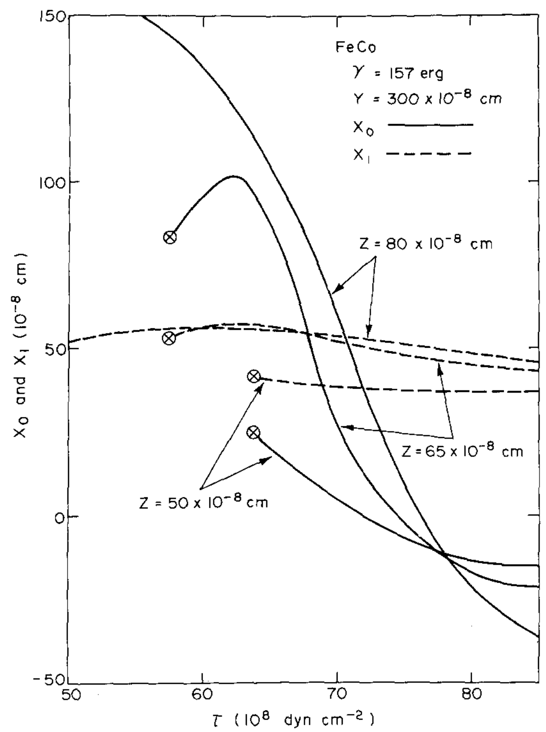

Figure 6 Variation of X_0 and X_1 with the applied stress for the constrained non-coaxial dislocation loops.

the loops generate disorder inside the crystal as discussed previously [19].

For a further understanding of the passing behaviour of the dislocation loops discussed with reference to $Y = 300 \times 10^{-8}$ cm (Fig. 4), X_0 and X_1 given by Equations 1 and 2 are represented as a function of the applied stress in Fig. 6. For $Z = 50 \times 10^{-8}$ cm, X_0 increases from some negative value while X_1 remains essentially constant. Cross-slip occurs by mode b, when X_0 is very nearly equal to X_1. For this configuration, the inner loops are closer to one another and, therefore, experience maximum cross-slip forces. Since during this decrease in stress, R_1 has also increased to a sufficient magnitude to force the cross-slip by mode b.

On the other hand, when $Z = 65 \times 10^{-8}$ cm, X_0 increases and reaches a maximum before it decreases. The decrease of X_0 means that the loops that are about to pass are snapped back to reform the dipole. This snapping is again related to the way the screw segments elongate during passing. When the loops are small, the passing stresses are also small since the internal stresses holding the dipole together are small. However, as the dipoles are about to break apart, the screw segments meanwhile increase their lengths thereby increasing their attraction forces which cause the loops to snap back to reform the dipole. During the snapping processes, however, cross-slip forces also increase proportionately leading to cross-slip and mutual annihilation of the screw segments.

When Z is increased to 80×10^{-8} cm, X_0 increases continuously while X_1 stays nearly constant. From Fig. 1b and c, such an increase of X_0 without a corresponding increase in X_1 corresponds to complete passing of the loops rather than to uncoupling. Since Z is larger than that considered above, the internal stresses between the loops are not sufficient either to hold the dipole or to snap back to reform the dipole that is being decomposed. The same results are obtained for $Y = 270 \times 10^{-8}$ cm.

The present investigation was originally motivated by the argument that since cross-slip of the dislocation loops is difficult, smaller separations between the passing dislocation loops could be obtained which could induce uncoupling of the dislocation loops and thus provide a mechanism for the generation of disorder in the crystal. The results obtained, however, indicate that the behaviour of the dislocation loops is somewhat similar to that of infinite dislocations. That is, if Z is amall, the dislocation cross-slip and annihilate their screw segments, and if Z is large, dislocations pass completely without any uncoupling. Although, cross-slip is relatively difficult for the loops, because of their flexibility to elongate preferentially along their screw orientation, cross-slip becomes an easier process compared to say uncoupling. Indeed, the presence of such elongated loops is a common feature in many ordered alloys [2–4]. While it is interesting to find out that the cross-slip as well as passing behaviour of dislocation loops closely follow that of infinite dislocations, the question still remains concerning the mechanism for the generation of disorder in ordered alloys.

It could be argued that the present analysis has considered only the effects of long range line tension on the cross-slip behaviour of loops. Superimposed over these effects, however, there could be additional short range line tension effects that would make the cross-slip process more difficult in comparison to passing and uncoupling. Furthermore, consideration of anisotropic frictional forces should make cross-slip even more difficult to accomplish. A detailed analysis of these aspects is required before further can be said about the mechanism of generation of disorder in single crystalline ordered alloys that are oriented for single slip.

5. Summary and conclusions

The behaviour of constrained non-coaxial superlattice dislocations loops has been determined by approximating the loops by piecewise segments. The purpose of the investigation was to determine whether or not the loops could uncouple during their passing thus generating disorder within the crystal. The results indicate that the loops either pass one another completely without any uncoupling or else elongate preferentially along their screw orientation until the internal stresses are sufficient for the loops to cross slip and mutually annihilate their unlike screw segments. Thus, the behaviour of the loops are found to be somewhat similar to infinite superlattice dislocations wherein cross slip or passing occurs in preference to uncoupling. It is suggested that additional analysis is required before more can be said concerning the mechanism of generation of disorder in single crystalline ordered alloys oriented for single slip.

Acknowledgements

The author expresses his appreciation to Professor M. J. Marcinkowski for many stimulating discussions concerning the various aspects of atomic ordering. The present research was supported by the United States Energy Research and Development Administration under contract no. AT-(40-1)-3935. The computer time for this investigation was made available through the facilities of the Computer Science Center of the University of Maryland.

References

1. M. J. MARCINKOWSKI, "Treatise on Materials Science and Technology", Vol. 5, edited by H. Herman (Academic Press, New York, 1974) p. 181.
2. G. LAKSO and M. J. MARCINKOWSKI, *Trans. Met. Soc. AIME* **245** (1969) 1111.
3. H. J. LEAMY, F. X. KAYSER, and M. J. MARCINKOWSKI, *Phil. Mag.* **20** (1969) 763, 779.
4. J. CZERNICHOW and M. J. MARCINKOWSKI, *Met. Trans.* **2** (1971) 347.
5. A. E. VIDOZ and L. N. BROWN, *Phil. Mag.* **7** (1962) 1167.
6. G. SCHOECK, *Acta Met.* **17** (1969) 147.
7. A. E. VIDOZ, *Phys. Stat. Sol.* **28** (1968) 145.
8. G. SCHOECK and E. PEREZ, *Scripta Met.* **5** (1971) 421.
9. M. J. MARCINKOWSKI and G. E. LAKSO, *J. Appl. Phys.* 38 (1967) 2124.
10. A. H. COTTRELL, "Dislocations and Plastic Flow in Crystals" (Oxford, London, 1953).
11. M. J. MARCINKOWSKI and K. SADANANDA, *J. Appl. Phys.* **45** (1974) 2441.
12. K. SADANANDA, in preparation.
13. K. SADANANDA and M. J. MARCINKOWSKI, *J. Appl. Phys.* **46** (1975) 18.
14. T. JOSSANG, J. LOTHE and K. SKYLSTAD, *Acta Met.* **13** (1965) 271.
15. T. JOSSANG, *Phys. Stat. Sol.* **27** (1969) 579.
16. T. JOSSANG and J. P. HIRTH, *Phil. Mag.* **13** (1969) 657.
17. M. J. MARCINKOWSKI and H. J. LEAMY, *Phys. Stat. Sol.* **24** (1967) 149.
18. K. SADANANDA and M. J. MARCINKOWSKI, *J. Appl. Phys.* **46** (1975) 27.
19. *Idem, Phys. Stat. Sol. a* **27** (1975) 141.

Received 19 March and accepted 14 May 1976.